Complementarity of Variable-magnification and Spectral-separation Fluorescence Imaging Systems for Noninvasive Detection of Metastasis and Intravital Detection of Single Cancer Cells in Mouse Models

YONG ZHANG[1], YUKIHIKO HIROSHIMA[1,2,3], HUAIYU MA[1], NAN ZHANG[1], MING ZHAO[1] and ROBERT M. HOFFMAN[1,2]

[1]*AntiCancer, Inc., 7917 Ostrow Street, San Diego, CA, U.S.A.;*
[2]*Department of Surgery, University of California, San Diego, CA, U.S.A.;*
[3]*Yokohama City University Graduate School of Medicine, Yokohama, Japan*

Abstract. *Imaging of tumor growth, progression and metastasis with fluorescent proteins in mouse models is a powerful technology. A limit to fluorescent-protein imaging has been for non-invasive deep-seated tumors, such as those in the lung. In the present study, the Maestro spectral-separation fluorescence imaging system and the OV100 variable-magnification imaging system were compared for noninvasive detection of metastasis in fluorescent protein-expressing orthotopic lung, liver, pancreas, and colon cancer in nude mouse tumor models, as well as for intravital single-cell imaging. Sensitivity, multispectral capability, contrast, and single cell resolution were investigated. The Maestro system outperformed the OV100 for noninvasive imaging of primary and metastatic tumors. The Maestro system detected brain tumor metastasis five days earlier than did the OV100. The Maestro had greater depth of detection compared with the OV100. By separating skin and food autofluorescence, the Maestro provided high-contrast images. The Maestro system was able to produce composite images with more unmixed components and detected more different color signals simultaneously than did the OV100. However, the OV100 system had higher resolution and was able to detect single cells in vivo unlike the Maestro. The present study demonstrates that the two instruments are complementary for imaging of all stages of cancer in mice, including single-cell trafficking and the superiority of in vivo fluorescent-protein imaging over luciferase imaging.*

Correspondence to: Robert M. Hoffman, Ph.D., AntiCancer, Inc., 7917 Ostrow Street, San Diego, CA 92111, U.S.A. Tel: +1 8586542555, Fax: +1 8582684175, e-mail: all@anticancer.com

Key Words: GFP, RFP, nude mice, human tumors, metastasis, imaging, noninvasive, variable magnification, subcellular in vivo imaging, spectral separation, tunable filter.

Fluorescent proteins are so bright that simple equipment can be used for *in vivo* imaging. Macro-imaging studies require equipment as simple as an LED flashlight with appropriate excitation filters and an emission filter for detection (1).

A fluorescence light box with fiber-optic lighting and appropriate filters, can be used to image tumors and metastasis that can be captured with a simple digital camera (2). Excitation with a narrow-band filter at approximately 490 nm should be used. Fluorescence emission can be observed through a 520 nm long-pass filter (2).

A powerful hand-held imaging device that inputs the image directly to a computer monitor can also be used (3).

However, for high-contrast deep imaging and single-cell *in vivo* imaging, more sophisticated instrumentation is needed. A variable-magnification small animal imaging system (OV100; Olympus Corp.), can be used for macro and subcellular imaging in live mice. The optics of the OV100 fluorescence imaging system have been specially developed for macroimaging, as well as microimaging, with high light-gathering capacity. The OV100 has lenses mounted on an automated turret with a high magnification range of ×1.6 to ×16 and a field of view ranging from 6.9 to 0.69 mm. Imaging of the entire mouse body down to the subcellular level is possible (4).

The use of tunable filters enables the separation of any individual spectrum within any fluorescent pixel (Maestro, CRi-PerkinElmer, Waltham, MA, USA). This technique can eliminate autofluorescence, and can enable high-resolution spectral distinction when multiple fluorescent proteins are being used. Spectral resolution thus presents the possibility of non-invasive imaging of tumors and metastasis in deep tissues (5).

The present report demonstrates the advantages of combining spectral separation to enhance fluorescent-protein imaging by eliminating interfering autofluorescence, thereby

enabling noninvasive imaging of deep tumors as well as variable-magnification imaging for *in vivo* visualization of single cells expressing fluorescent proteins.

Materials and Methods

Instrumentation. The OV100 Small Animal Imaging System (Olympus), containing an MT-20 light source (Olympus Biosystems) and DP70 CCD camera (Olympus) was used. High-resolution images were captured directly on a PC (Fujitsu Siemens, Munich, Germany). Images were processed for contrast and brightness and analyzed with the use of Paint Shop Pro 8 and CellR (Olympus Biosystems) (4).

The Maestro™ system, based on the use of a liquid crystal tunable filter (LCTF) for spectral separation, was also used (5, 6). The Maestro multispectral imaging system contains an LCTF optically coupled to a CCD camera. Multispectral images are acquired, with images typically spaced every 10 nm throughout the desired spectral range (6, 17).

Cancer cells. Red fluorescent protein/green fluorescent protein (RFP/GFP)/double-labeled Lewis lung carcinoma cells (LLC-RFP-GFP) (7, 8), MiaPaCa-2-RFP human pancreatic cancer cells (9, 10), SKHep-1-RFP human liver cancer cells (11), HCT-116-GFP human colonic cancer cells (12), and 4T1-RFP mouse breast cancer cells (13) (AntiCancer Inc., San Diego, CA, USA) were maintained in RPMI-1640 medium (Irvine Scientific, Santa Ana, CA, USA) supplemented with 10% fetal bovine serum, 2 mM glutamine (GIBCO/BRL, Life Technologies, Inc., Grand Island, NY, USA) at 37˚C in a CO_2 incubator (7, 14, 15).

Animals. Nude (*nu/nu*) mice (female, 6-7 weeks) (AntiCancer Inc.) were used. Mice were kept in a barrier facility under HEPA filtration (16). Mice were fed with autoclaved laboratory rodent diet. All animal studies were conducted with the AntiCancer Institutional Animal Care and Use Committee (IACUC)-protocol specifically approved for this study and in accordance with the principals and procedures outlined in the National Institute of Health Guide for the Care and Use of Animals under Assurance Number A3873-1.

Orthotopic organ tumor models. Subcutaneous tumors grown from the cells described above were harvested for surgical orthotopic implantation (SOI). The animals were anesthetized with a ketamine mixture (50% ketamine, 38% xylazine, and 12% acepromazine maleate). The surgical area was sterilized using iodine and alcohol. After proper exposure of the corresponding organ (lung, liver, colon, pancreas) following an incision, tumor fragments (1 mm^3) were implanted onto the corresponding organ (16). An 8-0 surgical suture was used to penetrate these small tumor pieces and suture them to the wall of the organ. The organ was then returned to the thorax/abdominal cavity. The incision in the abdominal wall was closed with a 6-0 surgical suture in one layer. For the thoracotomy procedure to implant tumor on the lung, the animals were kept under isoflurane anesthesia during surgery. For the other operations, the ketamine mixture described above was used for anesthesia. All procedures of the operation described above were performed under a ×7 magnification microscope (Olympus) (16).

Brain metastasis model. 4T1-RFP breast cancer cells (5×10^6 in 100 μl serum-free solution) were injected slowly into the right second mammary gland of a nude mouse. When the average tumor volume reached approximately 500-600 mm^3, the primary tumor was removed on day 18 after tumor implantation. Subsequent brain metastasis was observed with the OV100 and the Maestro fluorescence imaging systems (18).

Depth of detection. 4T1-RFP tumor tissue (3×3 mm^3) was placed at the bottom of a cell-culture dish. Pieces of mouse skin, harvested from the back of nude mice, were added on top of the tumor tissue, one layer at a time, up to six layers, to obtain different depths for imaging.

Skin flap imaging of single cells. Nude mice were anesthetized with the ketamine mixture described above *via s.c.* injection. An arc-shaped incision was made in the abdominal skin from the axillary to the inguinal region. The *s.c.* connective tissue was separated to free the skin flap without injuring the blood vessels. Mice were laid flat and the skin flap was spread and fixed on a flat stand. The blood vessel were exposed from the skin side. MiaPaCa-2 GFP-RFP dual-color cells (5×10^4 in 10 μl) were then injected into the epigastric cranialis vein through a catheter. Images were captured with the OV100 system (4).

Results and Discussion

Depth of detection. The Maestro system detected deeper tumors than did the OV100 when whole-body images were compared with the same mice. The Maestro system had greater depth imaging capability than the OV100 to detect brain metastasis (Figure 1). Noninvasive images obtained with the Maestro system had a significantly higher mean lung tumor signal over background (3.79 ± 0.5) compared to noninvasive images obtained with the OV100 (0.98 ± 0.22) ($p<0.01$). Open images taken obtained with the Maestro system had a significantly higher mean lung tumor signal over background (10.62 ± 1.4) compared to open images obtained with the OV100 (1.23 ± 0.24) ($p<0.01$) (Figure 2).

4T1-RFP tumor tissue (3×3 mm^3) was placed at the bottom of the cell culture dish (Figure 3 A). Pieces of mouse skin, harvested from the back of nude mice, were added on top of the tumor tissue one piece at a time up to six layers in order to obtain different depths for imaging. The Maestro system detected deeper tumor fluorescence signals through at least one more mouse-skin layer than did the OV100. The Maestro system had a larger signal-to-background ratio at different depths, and, therefore, better ability to resolve weak signals from deep tissues (Figure 3 B and C).

High-contrast imaging. 4T1-RFP lung metastasis was *ex vivo* imaged with the Maestro and the OV100 systems. Figure 4A and B demonstrate the appearance of a tumor on the lung with the OV100 and with the Maestro systems, respectively, before spectral unmixing was performed with the Maestro. Tumor signals overlapped with lung autofluorescence and background. Figure 4C shows a pseudo-colored composite image after spectral resolution with the Maestro system. Figure 4D-F show spectrally unmixed component images using the Maestro system.

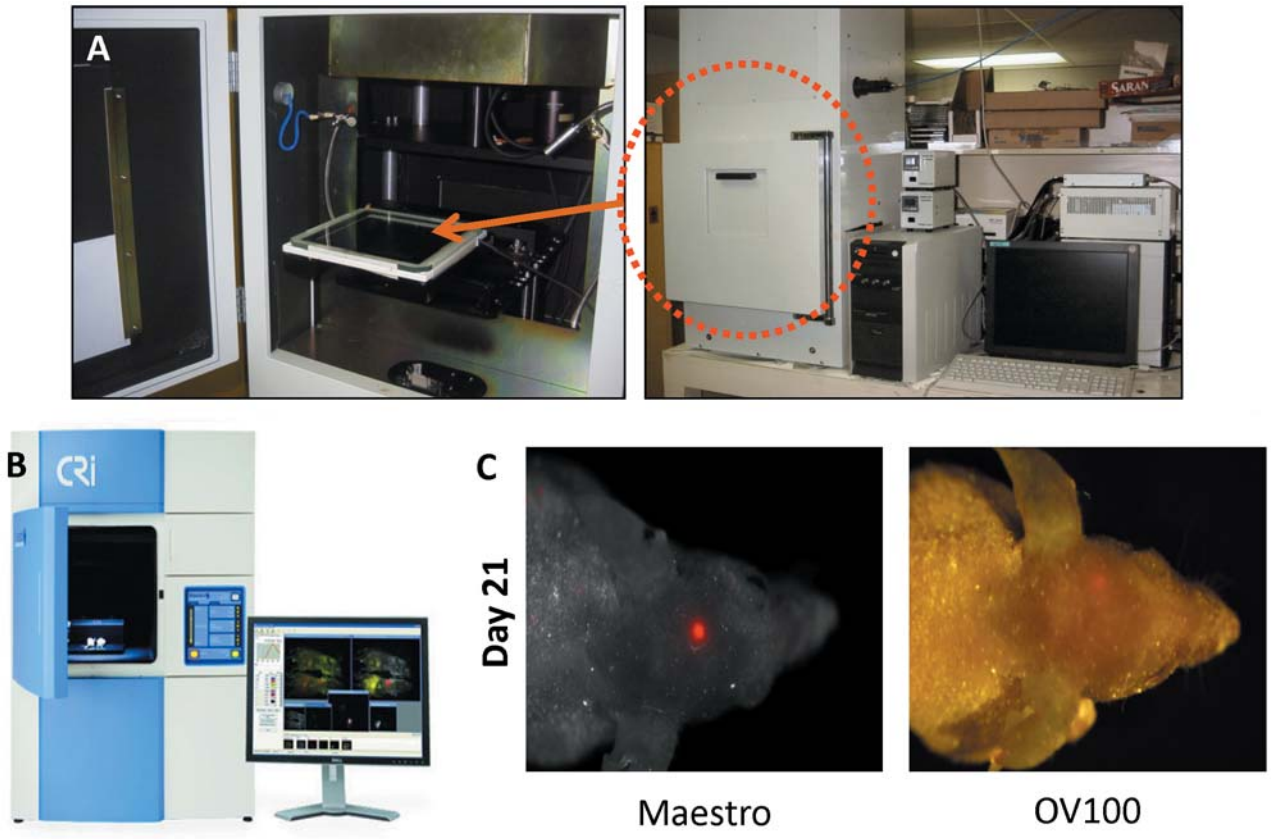

Figure 1. *Comparison of the OV100 and Maestro imaging systems: 4T1-red fluorescent protein (RFP) breast cancer cells (5 × 10^6/100 μl) in serum-free solution (100 μl) were injected slowly into the right second mammary gland of nude mice. When the average tumor volume reached approximately 500-600 mm^3, the primary tumor was removed on day 18 after tumor implantation. Subsequent brain metastasis was observed with the OV100 (Olympus Corp., Tokyo, Japan) and the Maestro (CRi-Perkin Elmer Inc., Waltham, MA, USA) fluorescence imaging systems. A: OV100 small animal imaging system. B: Maestro imaging system. C: Brain metastasis of 4T1-RFP imaged with the Maestro (left) and the OV100 (right).*

Multispectral imaging. Multiplexing with autofluorescence removal was performed on nude mice with different tumor models expressing GFP or RFP. The Maestro system was able to detect faint fluorescent signals separated from autofluorescence. The mice were implanted orthotopically with three types of tumors (SKHep-1-RFP liver cancer, HCT-116-GFP colon cancer, and MiaPaCa-2-RFP pancreatic cancer). The mice also had both skin and food autofluorescence. Four signals included: skin autofluorescence (pink); liver tumor and pancreatic tumor (red); colon tumor (green); and food (yellow). These signals were simultaneously generated by the CPS tool of the Maestro system (Figure 5A). The OV100 system was only able to image GFP and RFP simultaneously (Figure 5B).

Single-cell imaging. Using the OV100 system, MiaPaCa-2 dual-color cells, expressing GFP in the nucleus and RFP in the cytoplasm, trafficking in the vessels of a skin-flap, were imaged. MiaPaCa-2 dual-color cells were observed to migrate, elongate, divide, die, and extravasate from the vessel (Figure 6). Single cells could not be observed with the Maestro system.

The Maestro system was found to be more sensitive than the OV100 for detecting brain metastasis, which could be detected five days earlier with the Maestro than with the OV100 (Figure 1). The Maestro system was superior for depth of detection and high-contrast imaging compared to the OV100 (Figures 2, 3). The Maestro system demonstrated better multispectral capabilities compared to the OV100 (Figure 4). The Maestro system also allowed the separation of five or more fluorophores, with each signal quantitated and visualized separately (Figure 5). This is due to the LCTF of the Maestro system allowing spectral resolution.

The important advantage of the OV100 system is its ability to detect single cells *in vivo* in real time, whereby the cells were observed to elongate, divide, and die in a vessel or extravasate from the vessel (Figure 6). The optics of the OV100 fluorescence imaging system are specially developed for macroimaging, as well as microimaging, with high light-gathering capacity.

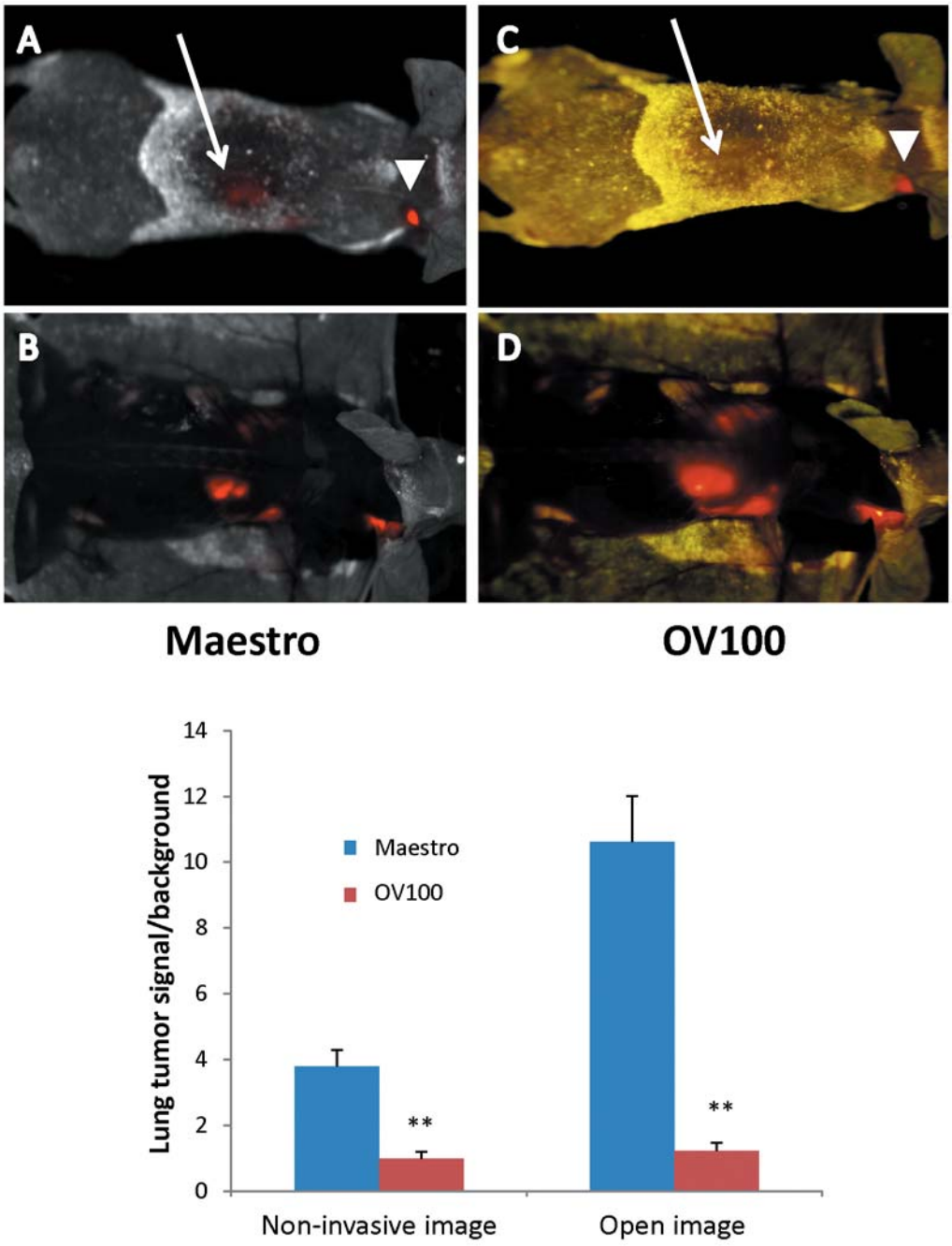

Figure 2. *Comparison of sensitivity of the OV100 and Maestro systems to detect the Lewis lung carcinoma-RFP on the lung. Images of the orthotopic Lewis lung-RFP tumor were obtained with the Maestro (A, B) and OV100 (C, D) systems. White arrow points to Lewis lung-RFP tumor; white arrowhead points to lymph node. (A and C are non-invasive images, B and D are open images). E: Signal to background ratio for non-invasive and open imaging by the Maestro and OV100. **p<0.01.*

Conclusion

For deep-tissue tumor fluorescence imaging, the Maestro spectral-separation instrument showed significantly better contrast than did the OV100. The Maestro system is more sensitive for noninvasive detection of brain or lung metastasis and has a superior signal-to-noise ratio compared with the OV100. The depth at which RFP fluorescence can be detected using the Maestro is significantly greater compared with the OV100. Multispectral imaging is also superior with the Maestro compared to the OV100. However, the OV100 has higher resolution and even single cells can be imaged, for example *via*

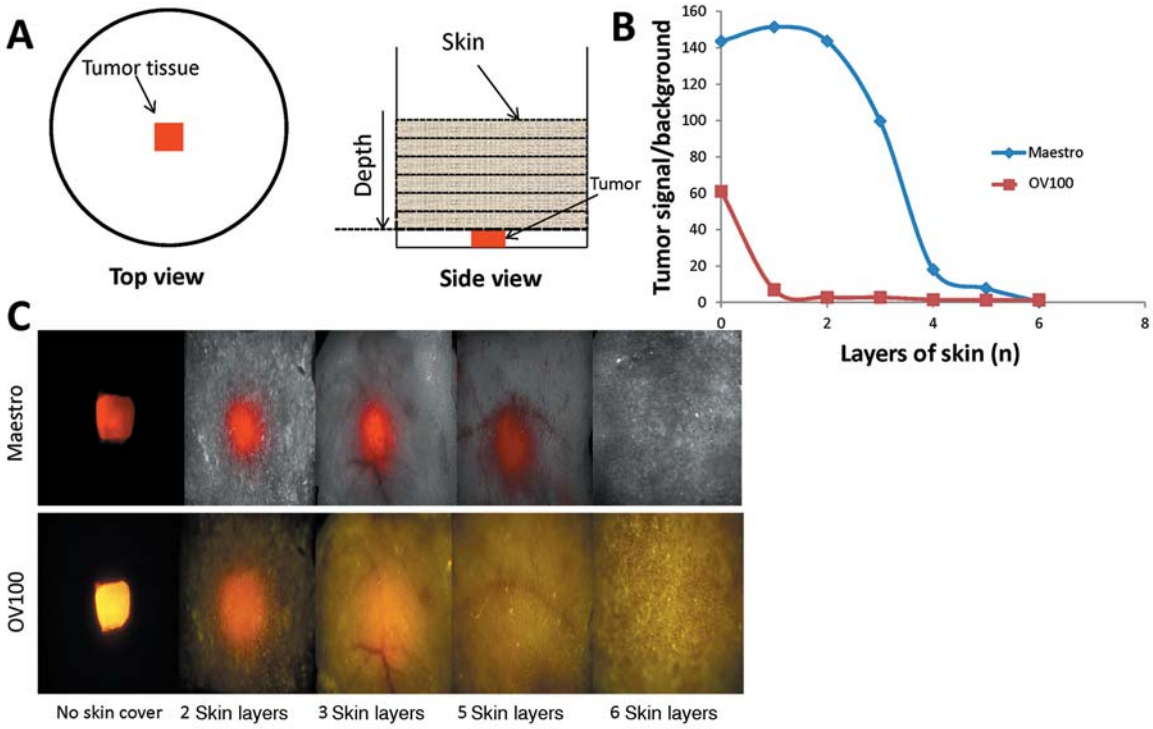

Figure 3. *Comparison of depth of OV100 and Maestro imaging of 4T1-RFP tumor tissue. 4T1-RFP tumor tissue fragments (3×3 mm^3) was placed at the bottom of a dish. Pieces of nude mouse skin were layered on the tumor, up to six layers. A: Depth of imaging was compared with the Maestro and OV100. B: Image contrast of the OV100 vs. that of the Maestro. C: Imaging of 4T1-RFP tumor tissue through skin layers. The top-row images were obtained with the Maestro, the lower-row images were obtained with the OV100.*

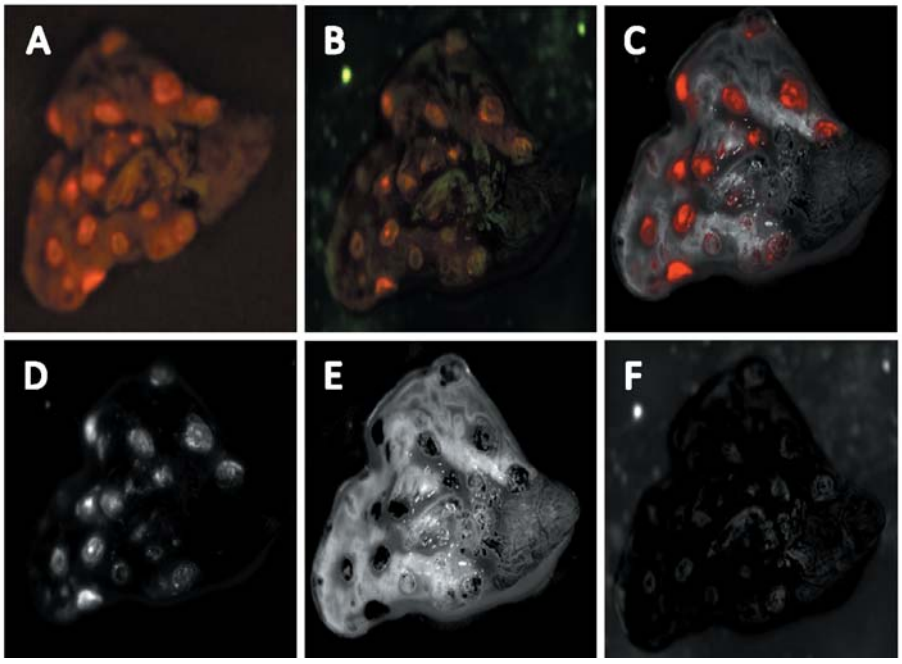

Figure 4. *Comparison of lung metastasis imaging with the Maestro and OV100 systems. 4T1-RFP lung metastases were imaged ex vivo with the Maestro and the OV100 systems. A: Image with the OV100. B-F: Images with the Maestro. B shows the appearance of the lung metastasis before spectral unmixing was performed with the Maestro. C: Pseudo-colored composite image. Tumor is red. D-F: Spectrally unmixed component images: D: tumor, E: autofluorescence, F: background signal.*

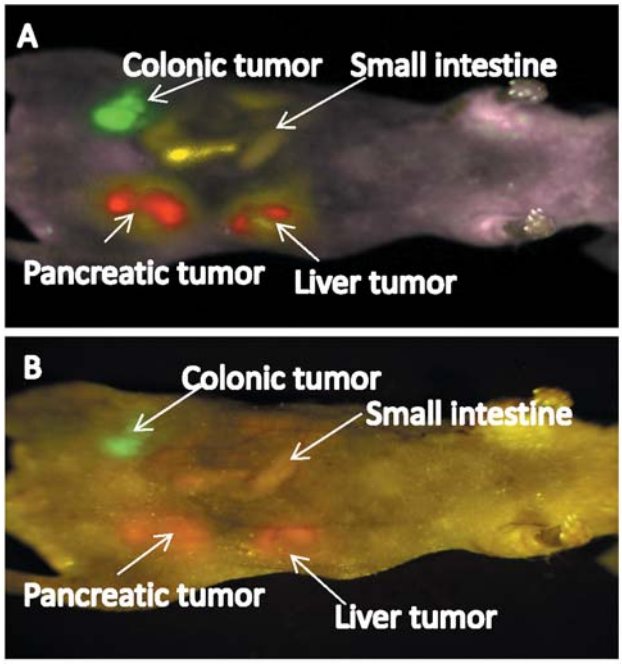

Figure 5. *Multispectral imaging with the OV100 and Maestro systems in nude mice. Nude mice with two different species of autofluorescence and three orthotopic tumors were examined. Mice were implanted orthotopically with the HCT-116-GFP colon tumor, SKHep1-RFP liver tumor and MiaPaCa-2-RFP pancreatic tumor and imaged with the Maestro and OV100 systems. A: Pseudo-colored composite image obtained with the Maestro. B: Image of the same mouse obtained with the OV100.*

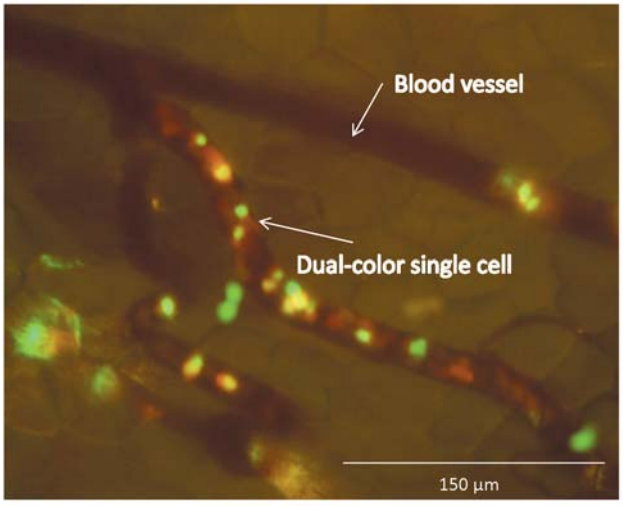

Figure 6. *Intravascular trafficking of dual-color MiaPaCa-2 human pancreatic cancer cells labeled in the nucleus with histone H2B-GFP and in the cytoplasm with RFP imaged with the OV100 system. See Materials and Methods for details.*

a skin-flap. The two instruments are complementary for *in vivo* imaging of cancer growth, progression and metastasis. The complementarity use of spectral resolution and variable-magnification imaging demonstrates the superiority of in vivo fluorescent-protein imaging over luciferase imaging (19).

Dedication

This paper is dedicated to the memory of A. R. Moossa, M.D.

Acknowledgements

This study was supported in part by National Cancer Institute grants CA CA132971.

References

1 Yang M, Luiken G, Baranov E and Hoffman RM: Facile whole-body imaging of internal fluorescent tumors in mice with an LED flashlight. Biotechniques *39*: 170-172, 2005.

2 Yang M, Baranov E, Jiang P, Sun F-X, Li X-M, Li L, Hasegawa S, Bouvet M, Al-Tuwaijri M, Chishima T, Shimada H, Moossa AR, Penman S and Hoffman RM: Whole-body optical imaging of green fluorescent protein-expressing tumors and metastases. Proc Natl Acad Sci USA *97*: 1206-1211, 2000.

3 Hiroshima Y, Maawy A, Sato S, Murakami T, Uehara F, Miwa S, Yano S, Momiyama M, Chishima T, Tanaka K, Bouvet M, Endo I and Hoffman RM: Hand-held high resolution fluorescence imaging system for fluorescence-guided surgery of patient and cell line pancreatic tumors growing orthotopically in nude mice. J Surg Res *187*: 510-517, 2014.

4 Yamauchi K, Yang M, Jiang P, Xu M, Yamamoto N, Tsuchiya H, Tomita K, Moossa AR, Bouvet M and Hoffman RM: Development of real-time subcellular dynamic multicolor imaging of cancer cell-trafficking in live mice with a variable-magnification whole-mouse imaging system. Cancer Res *66*: 4208-4214, 2006.

5 Levenson R, Yang M and Hoffman RM: Whole-body dual-color differential fluorescence imaging of tumor angiogenesis enhanced by spectral unmixing. Proc Am Assoc Cancer Res *45*: 46, 2004.

6 Mansfield JR, Gossage KW, Hoyt CC and Levenson RM: Autofluorescence removal, multiplexing, and automated analysis methods for *in vivo* fluorescence imaging. J Biomed Opt *10*: 41207, 2005.

7 Hoffman RM and Yang M: Subcellular imaging in the live mouse. Nature Protocols *1*: 775-782, 2006.

8 Rashidi B, Moossa AR and Hoffman RM: Specific route mapping visualized with GFP of single-file streaming contralateral and systemic metastasis of Lewis lung carcinoma cells beginning within hours of orthotopic implantation. J Cell Biochem *114*: 1738-1743, 2013.

9 Katz MH, Takimoto S, Spivack D, Moossa AR, Hoffman RM and Bouvet M: A novel red fluorescent protein orthotopic pancreatic cancer model for the preclinical evaluation of chemotherapeutics. J Surg Res *113*: 151-160, 2003.

10 Tran Cao HS, Bouvet M, Kaushal S, Keleman A, Romney E, Kim G, Fruehauf J, Imagawa DK, Hoffman RM and Katz MH: Metronomic gemcitabine in combination with sunitinib inhibits multisite metastasis and increases survival in an orthotopic model of pancreatic cancer. Mol Cancer Ther *9*: 2068-2078, 2010.

11 Gucev ZS, Oh Y, Kelley KM, Labarta JI, Vorwerk P and Rosenfeld RG: Evidence for insulin-like growth factor (IGF)-independent transcriptional regulation of IGF binding protein-3 by growth hormone in SKHEP-1 human hepatocarcinoma cells. Endocrinology *138*: 1464-1470, 1997.
12 Rajput A, Dominguez San Martin I, Rose R, Beko A, Levea C, Sharratt E, Mazurchuk R, Hoffman RM, Brattain MG and Wang J: Characterization of HCT116 human colon cancer cells in an orthotopic model. J Surg Res *147*: 276-281, 2008.
13 Ke C-C, Liu R-S, Suetsugu A, Kimura H, Ho JH, Lee OK and Hoffman RM: In vivo fluorescence imaging reveals the promotion of mammary tumorigenesis by mesenchymal stromal cells. PLoS One *8*: e69658, 2013.
14 Hoffman RM and Yang M: Color-coded fluorescence imaging of tumor-host interactions. Nature Protocols *1*: 928-935, 2006.
15 Hoffman RM and Yang M: Whole-body imaging with fluorescent proteins. Nature Protocols *1*: 1429-1438, 2006.
16 Hoffman RM: Orthotopic metastatic mouse models for anticancer drug discovery and evaluation: a bridge to the clinic. Investigational New Drugs *17*: 343-359, 1999.
17 Levenson RM and Mansfield JR: Multispectral in biology and medicine: Slices of life. Cytometry *69A*: 748-758, 2006.
18 Zhang Y, Miwa S, Zhang N, Hoffman RM, Zhao M. Tumor-targeting *Salmonella typhimurium* A1-R arrests growth of breast-cancer brain metastasis. Oncotarget, in press.
19 Kocher B, Piwnica-Worms D. Illuminating cancer systems with genetically engineered mouse models and coupled luciferase reporters in vivo. Cancer Disc 3: 616-629, 2013.

Received October 11, 2014
Revised November 1, 2014
Accepted November 4, 2014